LA-UR -87-3026

Los Alamos National Laboratory is operated by the University of California for the United States Department of Energy under contract W-7405-ENG-36

LA-UR--87-3026

DE88 000534

TITLE NEAR-REAL-TIME RADIOGRAPHY DETECTS 0.1% CHANGES IN AREAL DENSITY WITH 1-MILLIMETER SPATIAL RESOLUTION

AUTHOR(S) DAVID M. STUPIN, MST-7

SUBMITTED TO REVIEW OF PROGRESS IN NONDESTRUCTIVE TESTING
WILLIAMSBURG, VA
6/21-26/87

DISCLAIMER

MASTER

Los Alamos Los Alamos National Laboratory
Los Alamos, New Mexico 87545

NEAR-REAL-TIME RADIOGRAPHY DETECTS 0.1% CHANGES IN AREAL DENSITY WITH 1-MILLIMETER SPATIAL RESOLUTION

David M. Stupin
Materials Science and Technology Division
Los Alamos National Laboratory
Los Alamos, NM 87545

INTRODUCTION

Digital subtraction radiography serves angiography [1] and other medical applications successfully to extract minute x-ray signals from noisy backgrounds. Verhoeven [2] demonstrated that detecting surprisingly small changes in x-ray absorption makes this technique useful for industrial applications as well. I detect very small areal density differences and also wires as small as 2 μm in diameter although the spatial resolution of my x-ray apparatus is 1 mm.

Using digital subtraction radiography, I detect a 0.1% change in areal density in a phantom. Areal density is the product ρx, where ρ is the material density and x is the material thickness. Therefore, it is possible to detect a 0.1% difference in either density or thickness in unknown samples.

A special x-ray television camera detects the areal density change on the phantom. In a difference image, formed by subtracting the 128-television-frame averages of the phantom image from the phantom-and-step image, the step is resolved with a 1-mm spatial resolution. Surprisingly, crossed 2-μm-diam tungsten wires that overlie the phantom are also detected. This procedure takes a few seconds. The performance of any digital imaging x-ray system will improve by using the averaging and digital subtraction techniques

Beginning with the detection of both the 0.1% change in areal density and crossed 2-μm-diam wires, I hope to use digital subtraction radiography to detect areal density variations as small as 0.01% that are 1-μm wide.

DIGITAL SUBTRACTION RADIOGRAPHY

Digital subtraction radiography detects very small changes in an x-ray image by subtracting a background image from a foreground image. For flaw detection an x-ray image of a perfect part (the background

image) is subtracted from the image of the flawed part (the foreground image), leaving an image of only the flaw. For example, in digital subtraction angiography an x-ray image of a body is subtracted from an image of the same body that has an x-ray opaque solution injected into the blood stream, producing an image of the blood vessels. Both body images are stored digitally before subtraction. This latter technique can be a near-real-time process if the background image is stored in memory and subtracted from the foreground image as it becomes available. As in angiography, images can be extracted from very complex backgrounds.

Small areal density changes cause small changes in x-ray absorption. The noise in the image limits detection of very small changes in x-ray absorption. However, averaging video frames allows the detection of the smallest x-ray absorption changes by improving the signal-to-noise ratio of a digitized image. Digitally subtracting an averaged background image from an averaged foreground image removes fixed-pattern noise from the image. Inexpensive video image processors can average an input video signal and subtract it from a stored background image in a just a few seconds more than the time needed to average the images.

Furthermore, the recent introduction of several commercially available microfocus x-ray sources makes real time and digital subtraction radiography practicable for detecting small defects. Exceedingly small changes in x-ray absorption can be detected in near real time with a spatial resolution approaching that of x-ray film.

OPTIMAL X-RAY ABSORPTION

To detect such small changes in x-ray absorption, it is advantageous to use an x-ray energy for which the $\mu\rho x$ product is 1 to 3, where μ is the x-ray mass absorption coefficient (cm2/g) [3]. An anode with characteristic K-lines in the energy region below 25 keV can produce x-ray fluxes higher than those from the conventional tungsten anode [4,5]. For example, the x-ray flux from a molybdenum anode bombarded with 45-kV electrons is about three times more intense than the flux from a tungsten anode. Furthermore, nearly all x rays have the energies of the molybdenum K-lines between 17 and 20 keV. Therefore, very intense, nearly monochromatic sources can be generated. The 17 keV x rays from molybdenum and the 22-keV x rays from silver are very sensitive to absorption changes in my phantom.

The Phantom

To demonstrate the usefulness of the technique just described, I constructed a phantom that duplicates the absorption for 17-keV x rays in an integrated circuit with a plastic case (Fig. 1). It consists of stacked polyethylene sheets totaling 0.38 cm in thickness, 0.025-cm-thick aluminum, and 0.05-cm-thick silicon. In addition to these materials, aluminum circuits about 0.5-μm-thick are etched either into or on top of the integrated circuit's silicon wafer.

To detect very small absorption changes, I placed an aluminum step wedge over the phantom. Each step is 1 μm thick; the step thicknesses range from 1 to 12 μm. One micrometer of aluminum has 0.05% of the areal density in the phantom and absorbs 0.1% of 17-keV x-rays. Radiographers call x-ray absorption subject contrast. For comparison, the subject contrast of the phantom at 17 keV is 28 per cent. Figure 1 exaggerates the thicknesses of the aluminum circuits and the step wedge for clarity.

Digital Subtraction Imaging

The resultant images are formed by the method shown in Fig. 2. A 3-mA, 45-kV electron beam bombards a special water-cooled molybdenum anode in a microfocus x-ray source* to produce x rays that illuminate the sample phantom and step wedge. The x-ray image of the sample, magnified by 2x geometric projection, is cast onto a special x-ray television camera, which emits a signal that is digitized and averaged by a 512-by-512 pixel, 8-bit video digitizer.** The 128-frame averages travel to a computer (not shown) through an IEEE-48 interface. The computer subtracts the 128-frame average of the phantom image from the 128-frame average of the phantom-and-step image. The resultant image is transferred back to the frame grabber and displayed on a video monitor. This process takes a few minutes, but alternative ways to perform the same process in a few seconds are available.

Producing the molybdenum anode included depositing molybdenum [6,7] on a copper anode the same size as the tungsten anode supplied by the manufacturer. In addition to the copper construction, boring out the inside of the anode and inserting a water-cooling line improved the anode's heat-dissipating characteristics.

The special x-ray television camera is a phosphor-coated fiber optic train butted to a silicon-intensifier-target (SIT) television camera (Fig. 3). One hundred fifty micrometers of Gd_2O_2S:Tb coat a removable fiber optic faceplate 40 mm in diameter. Optical grease physically couples this faceplate to a tapered fiber optic with ends 40 and 18 mm in diameter. The 18-mm end joins to the bare front face of a SIT tube mounted in a standard SIT camera. The fiber optic train and shielding protect the camera's electronics from front-illuminating x rays with energies up to 50 keV. The removable, coated faceplate facilitates changing x-ray phosphors.

Although averaging 128 video frames, the maximum number imposed by the equipment, improves the signal-to-noise ratio in the image, fixed-pattern noise and camera-caused shading errors remain. Moreover, diminishing these errors by forming the difference of two average images does not eliminate some residuals.

AREAL DENSITY CHANGE DETECTION (0.1%)

Photographs of the television monitor show difference images of the phantom and step wedge and of the crossed 2-μm-diam tungsten wires (Figs. 4, 5, and 6). Figure 4 is the step wedge image at 2x magnification and a map of the image; the step wedge is slightly darker at the top because of

the x-ray camera's shading characteristics. The stretched contrast in Fig. 4 clearly shows the image of the first step as it emerges from the background noise. Aluminum steps are vertical with the thinnest step on the left and the thickest step on the right. Two pointers at the top and bottom mark the 1-μm-thick edge of the step wedge. By chance, a 2-μm-diam wire in the subtracted background image coincides exactly with the pointers. Therefore, I estimate that the second step, which is a 0.1% areal density change, is detected from the background. I estimate that this image has 1-mm spatial resolution; hence the individual 0.4-mm-wide steps are not resolved. Two horizontal black lines at the top of the image are 20- and 30-μm-diam tungsten wires. Line (a-a) shows the position of the video trace in Fig. 5.

Figure 5 shows the detection of the step wedge as it emerges from the background. It is a video trace across line (a-a) in the previous figure. Arrows (a) mark the beginning of the step wedge, that is, the location of the 1-μm-thick step of aluminum. The step wedge is 12 μm thick between arrows (b) and (c). The dip in the trace at arrows (a) is due to the wire in the subtracted image. The dashed line drawn through the data is an estimate of the noise-averaged signal and shows the detection of the 0.1% areal density change (the second step) in the sample. The slope of this estimate to the left of (a) and to the right of (c) is caused by the camera's shading characteristics.

In Fig. 6 a map explains a photograph of crossed 2-μm-diam tungsten wires that overlie the phantom. Unfortunately, these two wires are so faint that they probably will not appear in the published version of this figure. However, the 6-μm-diam wires are clearly visible. In the original appear five horizontal wires with diameters of 30, 20, 12, 6, and 2 μm and four vertical wires with diameters of 20, 12, 6, and 2 μm. Aluminum foils 20 and 12 μm thick cover the lower right corner. This corner is cluttered because contrast stretching, used to clarify the smallest wire, has destroyed both the shading of the foils and the detection of the wires over the foils. Two micrometers of tungsten absorb about 80% of 22-keV x rays; hence, 2-μm-wide lines with 80% absorption can be detected.

HIGH SENSITIVITY AND THE ADVANTAGES OF REAL TIME

A distinction must be made between the detection and the resolving powers of a detector system. Although crossed 2-μm-diam wires are detected in one image, the spatial resolution is not 2 μm. If two parallel wires of this diameter were separated by their diameter, they would not be resolved in these images. However, their presence would be detected. (Feldkamp [8] notes a similar result.) Sometimes this presence is sufficient to identify a faulty sample or to locate the position of an internal part.

Currently, digital subtraction radiography detects 0.1% variations in the areal density. Hence, 0.1% areal density variations can be detected in near real time. For these tiny variations, spatial resolutions as small as 1 mm are typical. However, linear features as narrow as 2 μm with 80% absorption can be detected but not resolved. The

performance of any digital-imaging x-ray system will improve by using the averaging and digital subtraction techniques.

The sensitivities just described can be obtained with samples that have an optimal x-ray examination energy of 1 to 20 keV (2 to 50 kV) by changing the anode material to select an appropriate K-line. This energy range is optimal for a wide variety of manufactured plastic and ceramic parts, such as 0.001- to 7-cm-thick samples of polystyrene or polyethylene. Furthermore, the work of Verhoeven at 75 kV suggests that similar results occur at energies above 50 kV with commercial x-ray image intensifiers.

ACKNOWLEDGMENTS

I thank Grant H. Stokes for many useful discussions and experiments; Norman E. Elliott for writing the software for the image processing; Lutz Dahlke of Sandia National Laboratories, Livermore, California, for many helpful discussions and for suggesting several important references. I also thank Gary Reeves for fabricating the aluminum step wedge, Elfino Armijo for fabricating the anode and other parts, P. Roger Lagasse for designing many of the components used in this experiment, Veronica Gomez for fabricating the wire-resolution targets, John Ben Cole for his help in the laboratory, and Faith J. Harp for editing the paper.

*Scanray MF-160. TFI Corporation, P.O. Box 1611, New Haven, CT 06506.

**Quantex DS-20. Quantex Corporation, 252 N. Wolfe Road, Sunnyvale, CA 94086.

+PDP-11/23. Digital Equipment Corp., Maynard, MA 01754.

REFERENCES

1. M. Paul Capp, Sol Nudelmar, Donald Fisher, Theron W. Ovitt, Gerald D. Pond, Meryl M. Frost, Hans Roehrig, Joachim Seeger, and Donald Oimette, "Photoelectronic Radiology Department," in Digital Radiography, William R. Brody, Ed. (SPIE, Bellingham, Washington, 1981), Vol. 314, pp. 2-8.
2. Leon Verhoeven, "Comparison of Enhancement Capabilities of Film Subtraction and Digital Subtraction Methods," in Digital Radiography, William R. Brody, Ed. (SPIE, Bellingham, Washington, 1981), Vol. 314, pp. 114-120.
3. Robin P. Gardner and Ralph L. Ely, Jr., Radioisotope Measurement Applications in Engineering (Reinhold Publishing Corporation, New York, 1967), p. 282.
4. J. V. Gilfrich, "Spectral Distribution of X-Ray Tubes," in Handbook of Spectroscopy, J. W. Robinson, Ed., (CRC Press, Boca Raton, Florida, 1974), Vol. 1, pp. 232-237.

5. D. B. Brown and J. V. Gilfrich, "Measurement and Calculation of Absolute X-Ray Intensities," J. Appl. Phys. 42 (10), 4044-4046 (1971).
6. D. W. Carroll, W. J. McCreary, "Fabrication of Thin-Wall, Free-standing Inertial Confinement Fusion Targets by Chemical Vapor Deposition," J. Vac. Sci. Technol. 20 (4), 1087-1090, (1982).
7. W. J. McCreary, D. W. Carroll, "CVD Techniques Applied to Energy Problems," in Proceedings of the Eighth International Conference on Chemical Vapor Deposition, CVD-III, Gouviex, France, September 15-18, 1981 (The Electrochemical Society, Pennington, New Jersey, 1981), Vol. 81-7, pp. 769-781.
8. L. A. Feldkamp, Ford Motor Co., Dearborn, MI 48121, private communication, June 1987.

FIGURE CAPTIONS

Fig. 1. An integrated-circuit phantom duplicates x-ray absorption in a plastic-case integrated circuit. The logarithm of the absorption is shown. Absorption of the aluminum circuits and the first step of the step wedge (neither shown to scale) is about 0.1% of the phantom.

Fig. 2. Digital subtraction radiography. The difference of two 128-frame averages produces images of objects with areal density changes as small as 0.1% and of 2-μm-diam wires with larger absorption.

Fig. 3. The x-ray television camera is a phosphor-coated, fiber optic faceplate optically coupled to a tapered fiber optic faceplate that is, in turn, coupled to a SIT television tube. Shielding on the front of the camera and the faceplates protect the camera electronics from low-energy x rays.

Fig. 4. Left: A contrast-stretched image of a step wedge that shows the detection of a 0.1% areal density change over the integrated-circuit phantom. Right: A map showing the location of the wedge and other objects. Two pointers indicate the edge of the 1-μm step. Line (a-a) locates the video trace in Fig. 5.

Fig. 5. A video trace across the step wedge shows the detection of the second step. Arrows (a) mark the beginning of the first (1-μm) step. Arrows (b) mark the 12-μm step. The region between (b) and (c) is 12 μm thick. The image of a 2-μm-diam wire in the subtracted background image coincides exactly with arrows (a). Dashed line is an estimate of the noise-averaged signal.

Fig. 6. Left: Crossed 2-μm-diam tungsten wires (black lines) detected over the integrated circuit phantom. Right: A map of the wires and other objects. In addition to the 2-μm wires are crossed wires 6, 12, and 20 μm in diameter.

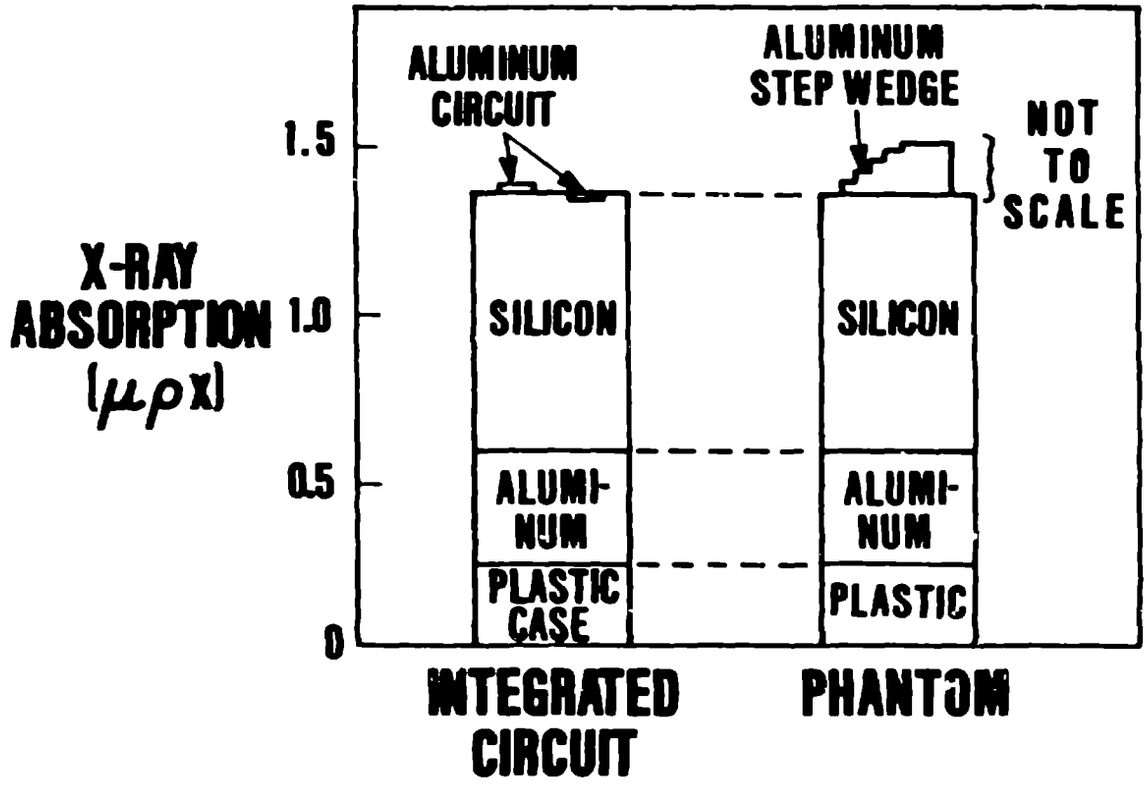

Los Alamos

Fig. 1

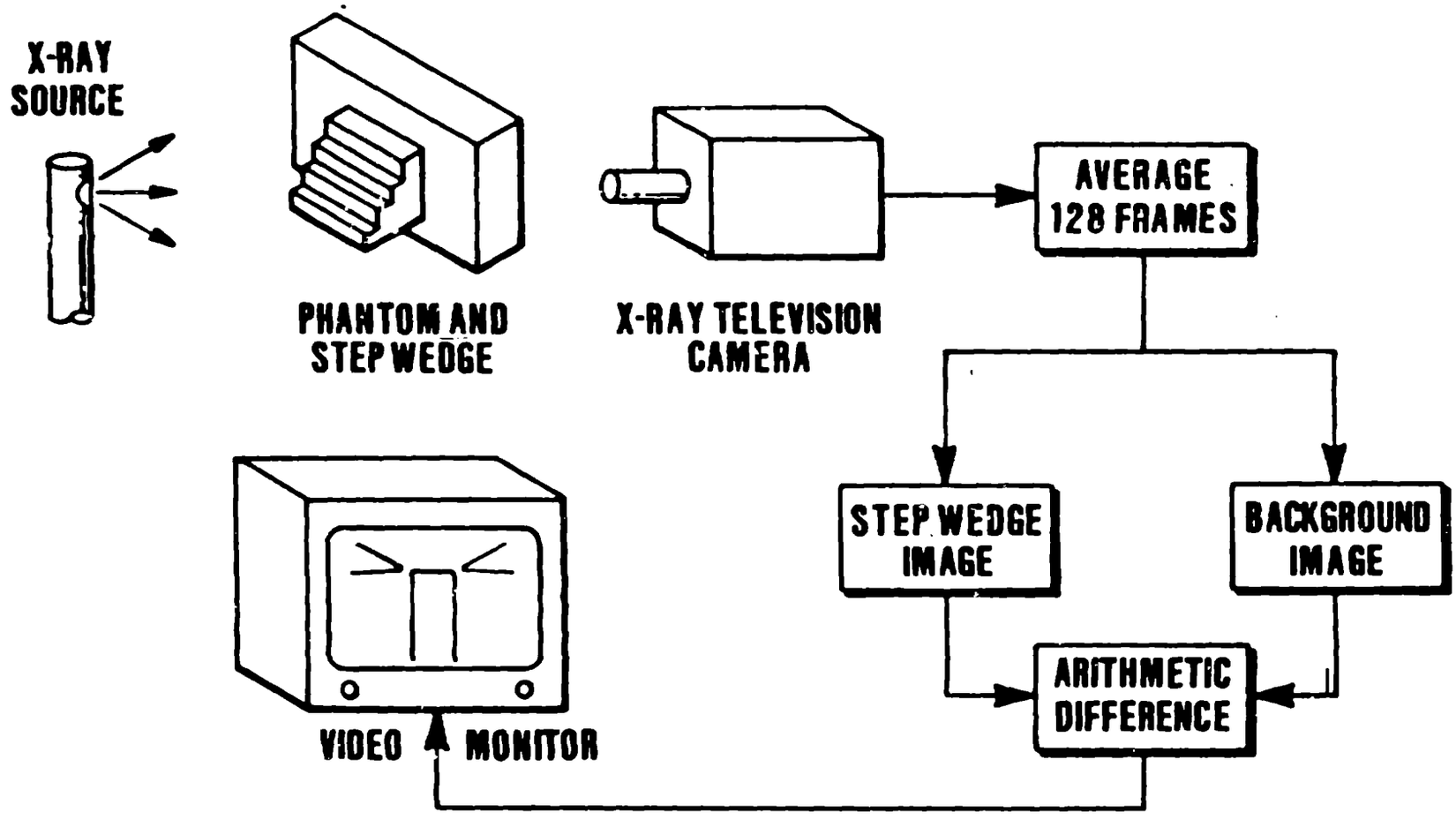
X-RAY SOURCE
PHANTOM AND STEP WEDGE
X-RAY TELEVISION CAMERA
AVERAGE 128 FRAMES
STEP WEDGE IMAGE
BACKGROUND IMAGE
ARITHMETIC DIFFERENCE
VIDEO MONITOR

Fig. 2

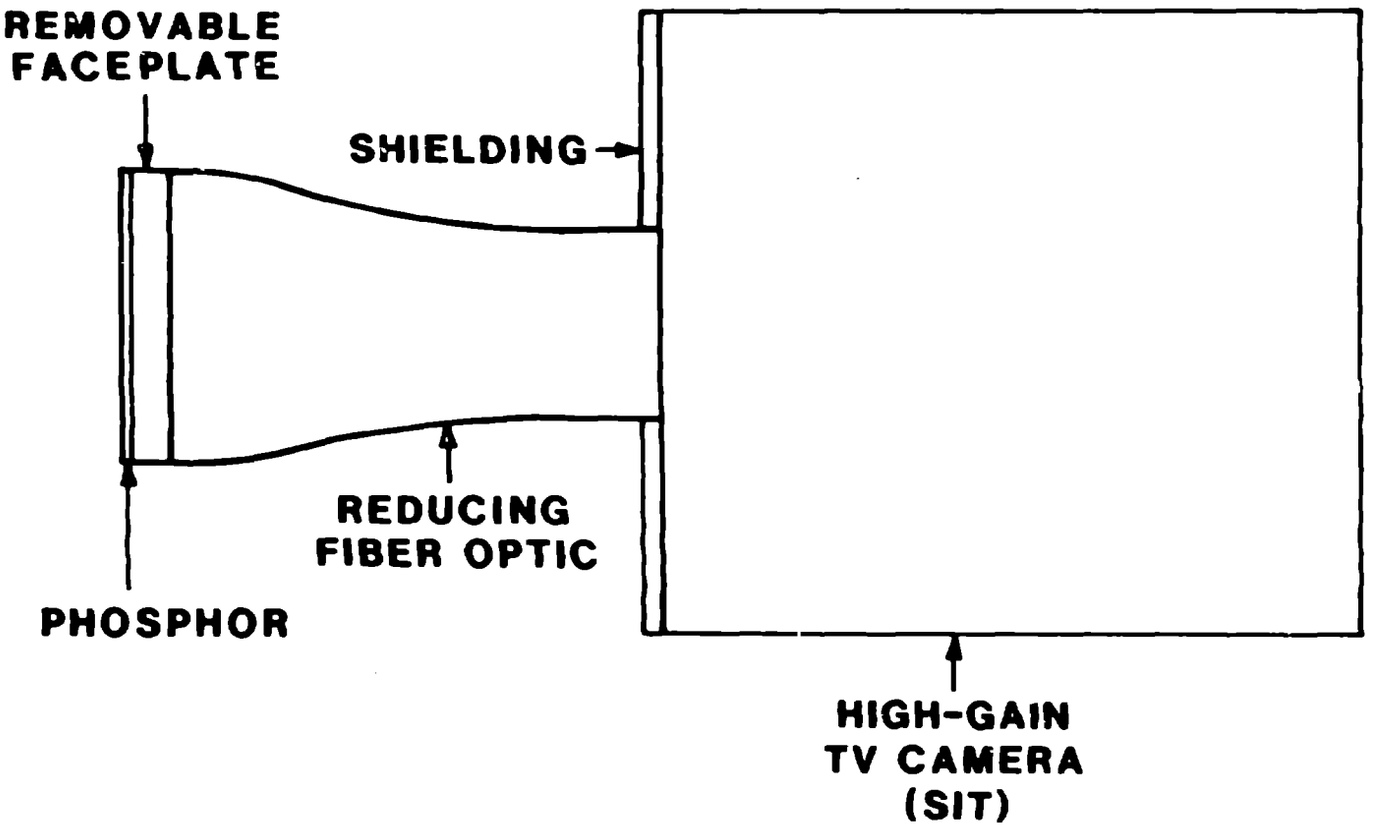
REMOVABLE
FACEPLATE
SHIELDING
REDUCING
FIBER OPTIC
PHOSPHOR
HIGH-GAIN
TV CAMERA
(SIT)

Fig. 3

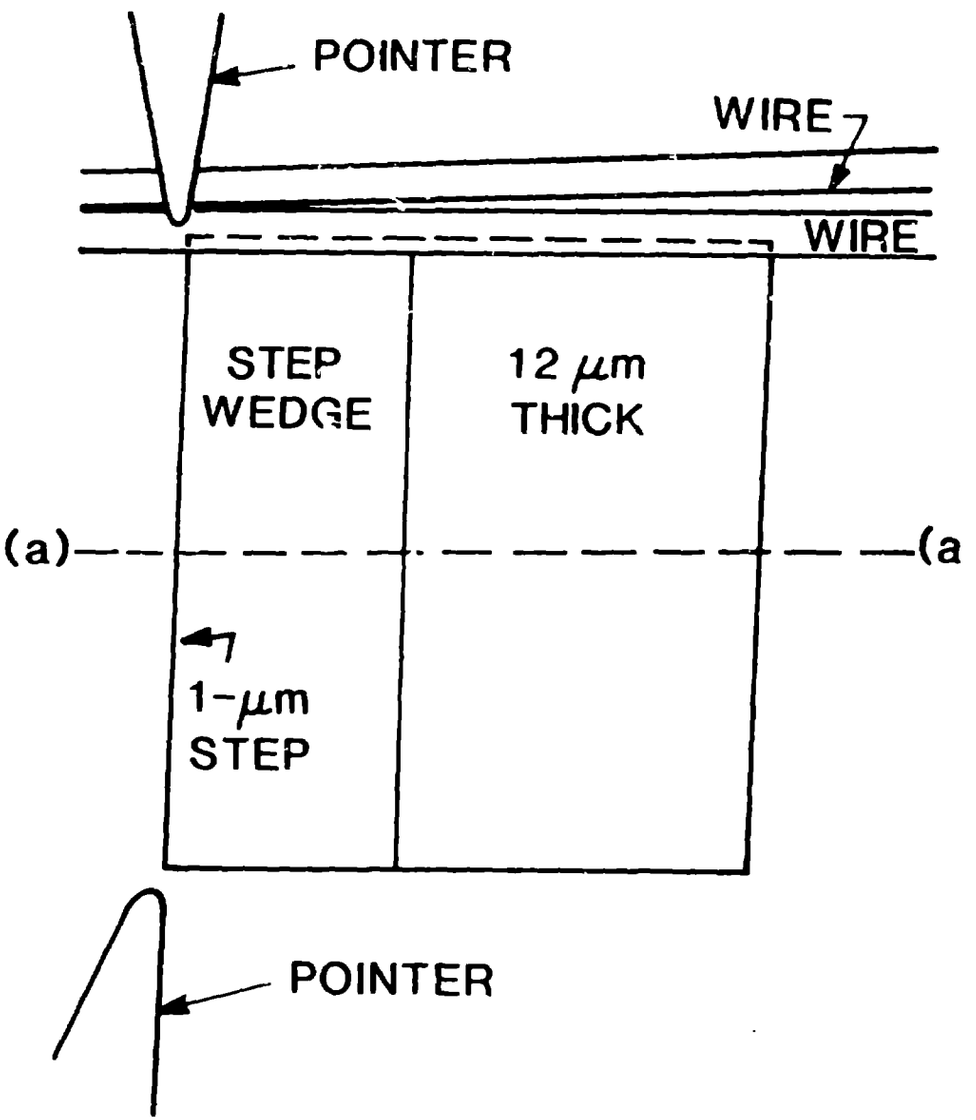

Fig. 4

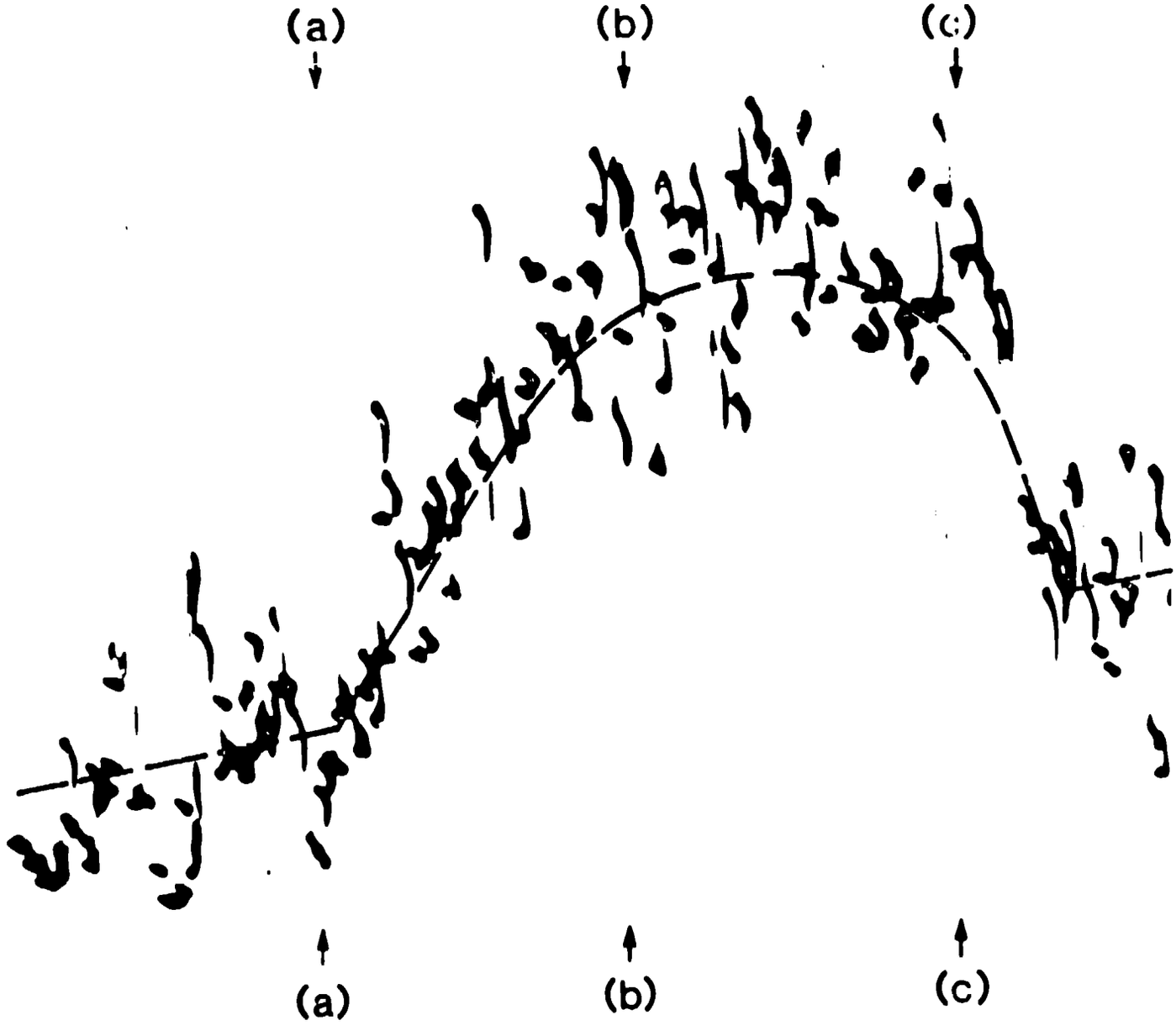

Fig. 5

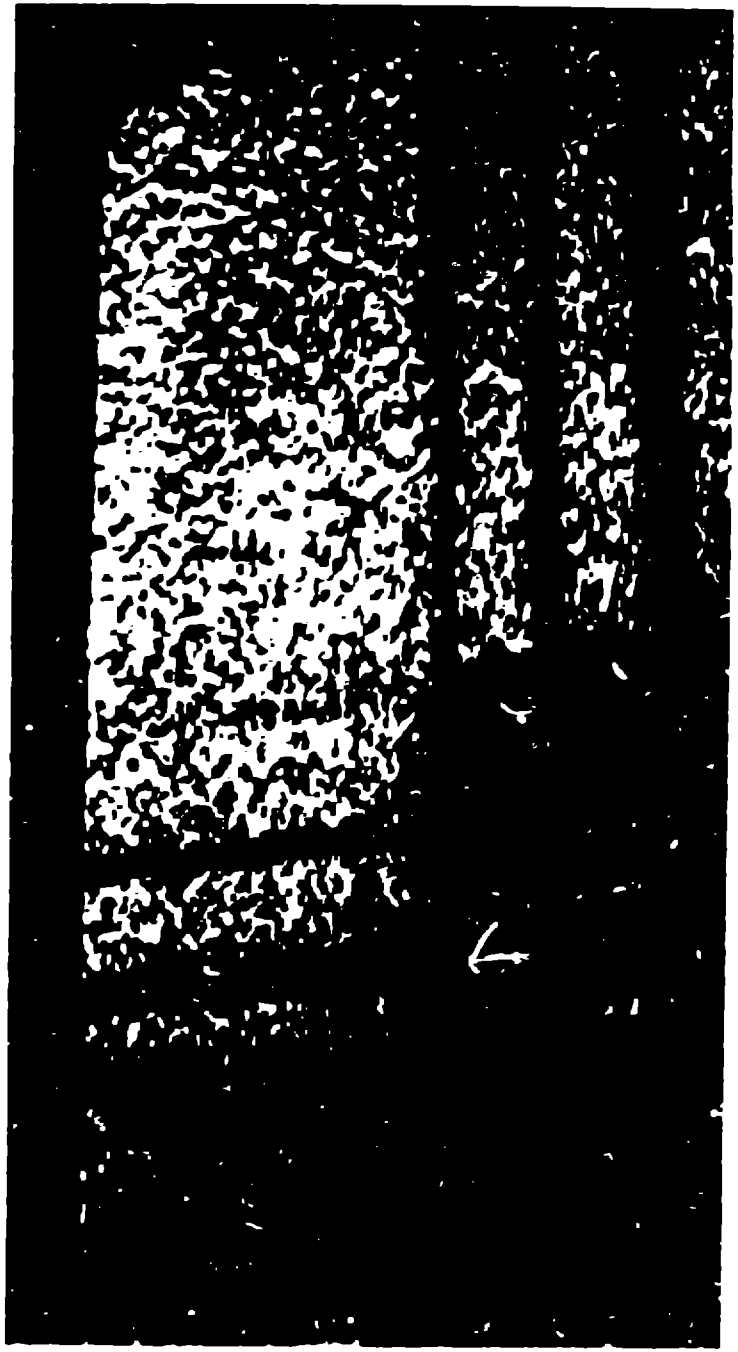

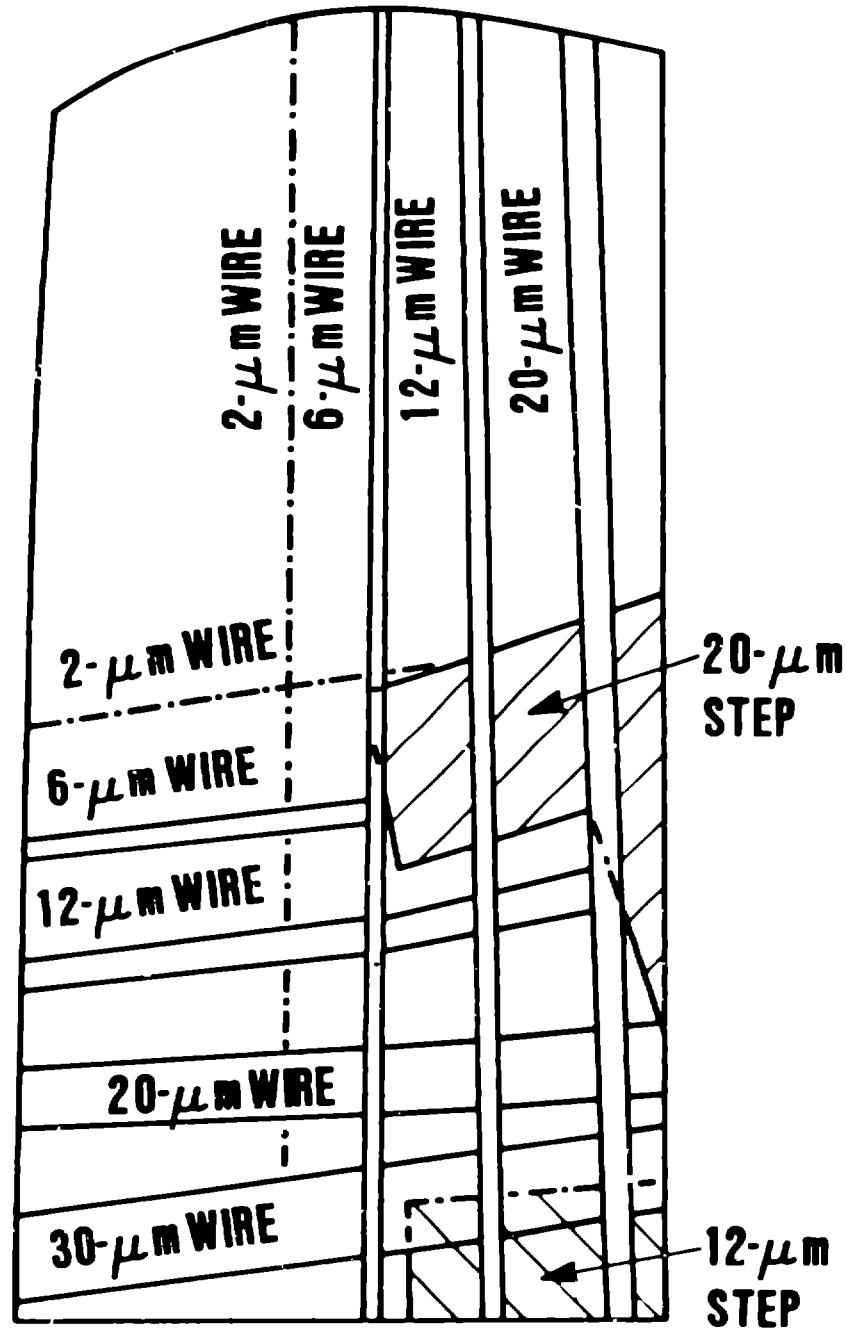
2-μm WIRE
6-μm WIRE
12-μm WIRE
20-μm WIRE
2-μm WIRE
6-μm WIRE
12-μm WIRE
20-μm WIRE
30-μm WIRE
20-μm STEP
12-μm STEP